A Blind Search for Variable Stars using an 11-inch RASA and a One-Shot Color Camera

Nathan Taulelei
Tristan Wood
Andrew Yen
Eltham College, 1660 Main Road, Research, VIC 3095, Australia; natanotau@gmail.com; tristanjtwood@gmail.com; ayen@elthamcollege.vic.edu.au

Michael Fitzgerald
Las Cumbres Observatory, 97 Dalton Street, Eltham, VIC, 3095, Australia; psyfitz@gmail.com

Lindsay van der Pal
Eltham College, 1660 Main Road, Research, VIC 3095, Australia; lindsay.vanderpal@gmail.com

Received June 20, 2023; revised January 30, 2024; accepted February 19, 2024

Abstract In this paper we report tests of an 11-inch wide field Rowe Ackermann Schmidt Astrograph (RASA), a one-shot color (OSC) imager and data processing semi-autonomously by ASTROSOURCE as a variable-hunting system. The success of this test is demonstrated by blind recovery of five known variables in the field, and identification of six more probable variables. The researchers repeatedly imaged and studied a single field of approximately three square degrees (March to June 2021) chosen based on the relative absence of AAVSO database stars within the field. Analysis techniques were developed and applied to process the large quantity of data produced to identify stars exhibiting variability over the time period. Twelve variable stars were identified, six previously known—albeit one with a curious period difference—and five potential, but not confirmed, discoveries (1 likely rotational, 1 likely RRc, 1 likely δ Scuti, and 2 of uncertain types). Some candidate stars were followed-up with further data obtained with a 0.4-m class telescope from Las Cumbres Observatory. The methods developed by this team to find and identify variable stars have proved efficient and productive. The potential discoveries were made on the dim end of the magnitude range (14th–16th), however, the exposure times used in this study were quite short and could reasonably be extended, so future searches will be made with longer exposures to focus on this magnitude range. Recommendations are made for future variable search using a combination of RASAs and OSCs.

1. Introduction

Variable star observations are primarily conducted by non-professional astronomers who have the physical and time resources to make patient time-series observations and measurements. Although large scale surveys such as TESS (Transiting Exoplanet Survey Satellite) are identifying thousands of candidate variable stars in their search for exoplanets (Waagen 2022), there is still scope for discovery by non-professional, earth-based survey techniques. Algorithmic analysis techniques have been developed and are widely used to identify variable stars within large CCD datasets (Breus 2017). A simple algorithmic technique measures each star in a field image (by comparing to comparison stars in the same image). The standard deviation of the measurements for a fixed brightness star is expected to increase with increasing magnitude; but stars that exhibit greater standard deviation than their similar magnitude siblings are tagged for follow-up and manual analysis. This technique is described by Breus (2017) however these researchers have adapted the method, using under-sampled OSC images for reasons given in the data analysis section.

Students at Eltham College, in Victoria, Australia, have access to robotic telescopes located on campus as well as the resources of Las Cumbres telescope network (https://lco.global/). This study was primarily driven by secondary student researchers.

2. Instruments and methods

The primary survey instrument was an 11-inch (280 mm) Rowe Ackermann Schmidt Astrograph (RASA) with a One-Shot Color (OSC) CMOS imager, a ZWO ASI071MC Pro. This instrument has a fast focal ratio and wide field, attributes that made it ideal for this type of survey. Typical exposures of 60 seconds yielded useful data across a field roughly 2.1° × 1.4° for stars down to 15th and 16th magnitude with a saturation at around 10th magnitude. The imager was 14 bit with a resolution of 4944 × 3284, yielding a pixel scale of 1.59"/px. The instrument is located at Eltham College on the Eastern fringe of Melbourne, Australia, with Bortle 4 skies (Bortle 2001). The OSC imager contains a Bayer matrix of filters—effectively imaging in red, green, and blue bands simultaneously. However, the three colors do not correspond well with standard filters, so it was decided to mathematically reduce the data to a "V" composite. This has been useful for identifying variability in stars in this field (the purpose of this survey) but it means this data are not directly comparable with photometry results taken through standard filters.

The follow-up instruments were the 0.4-m telescopes in the Las Cumbres Observatory network (Brown *et al.* 2013). This network is a not-for-profit science institution that provides access to a global network of robotic telescopes in both

northern and southern hemispheres. The researchers used 0.4-m telescopes in the network for follow-up observations in Siding Springs (Australia), Sutherland (South Africa), and Cerro Tololo (Chile). The SBIG STL6303 cameras on the 0.4-m telescopes have smaller fields of view (29 arcminutes × 19 arcminutes) but are equipped with standard photometric filters, including Sloan i' and Johnson V.

The data analysis techniques used were a critical tool in this survey. The field contained roughly 5000 stars per image (8198 was the maximum amount detected, 3 sigma above the background, in the best image) mostly brighter than 16th magnitude, and was imaged by the RASA 11-inch and the OSC camera 612 times, out of which 543 images were suitable to use. The data analysis allowed the researchers to identify candidate stars with variability significantly higher than the modal standard deviation of brightness in the stars with similar magnitude.

A purpose of this survey was to identify previously unknown variable stars utilizing a method based on finding stars above a certain amount of variation above the mean variation within a binned magnitude. The particular tool used in this research was AstroSource (Fitzgerald *et al.* 2021), however there are many other packages that take similar approaches (e.g. C-Munipack: https://c-munipack.sourceforge.net/ (Motl 2011)). A field was chosen that met a number of criteria including a paucity of known variable stars in the AAVSO databases. The researchers set the following criteria (Stamp 2016): accessible to Eltham College observatory telescopes (below 20° S Declination); no bright stars (magnitude < 4) within the field; a low quantity of known variable stars within the field; close to, but not within the galactic plane (Milky Way) to provide a high density of stars to search through.

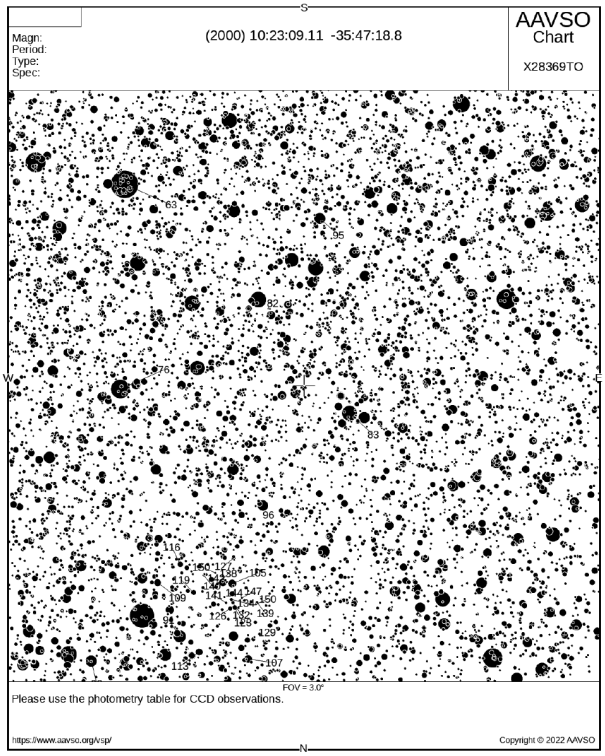

Figure 1. AAVSO finder chart of the field of view chosen.

The researchers selected a region in Antlia that met the criteria. The selected region is shown in Figure 1—an extract from the AAVSO Variable Star Plotter (VSP) chart function. The relative density of higher magnitude (dimmer) stars and absence of low magnitude (bright) stars in the field is apparent.

3. Observations

Over 14 nights between March and May 2022, 612 exposures were taken with the OSC on the 11-inch RASA. The exposure time was 60s for most of the exposures, with 52 20s exposure times in the first three observing nights. This information is summarized in Table 1.

Table 1. RASA Survey summary.

Observation period	*Number of observation nights*	*Number of field images taken*	*Exposure*
March 31–May 29, 2022	14	612 (543 used in analysis)	60s (20s for first 3 nights)

4. Data analysis

4.1. Reduction

The raw data from the RASA OSC were bias-, dark-, and flat-corrected by the OSS Pipeline (Fitzgerald 2018). Photometry was performed using Source Extractor Kron aperture photometry (Bertin and Arnouts 1996). AstroSource (Fitzgerald *et al.* 2021) was used to process and analyze the resulting photometry. While PSF methods were available and are usually better, the blockiness of the pixel scale of the OSC prevented an adequate PSF model to be fit. As the camera was a one-shot color camera as opposed to a traditional monochrome CCD camera, three approaches to manipulating the Bayer data were trialled to attempt to squeeze out the best photometry that was possible with the hope that some color information could be retained.

4.2. Internal photometry

The first approach was to take the Bayer grid and create separate B, G, and R interpolated images that retained the same pixel scale; hence 3 pixels for B and R, and 2 pixels for G were "fake" filled-in pixels estimated from the surrounding data. The second approach was to take the Bayer grid and simply collapse the grid down to an image for each color that represented double the pixel scale but involved no interpolation, representing all "real" measurements—two "real" pixels per collapsed pixel for Green and one "real" pixel per collapsed pixel for Blue and Red. The third approach was to ignore the color information entirely and simply bin the entire Bayer grid 2 × 2 into a single image with double the pixel scale. These three approaches are visually represented in Figure 2.

The first approach involving interpolation was attempted both with the Menon *et al.* (2007) method, which uses information from pixels of the other colors to provide better approximation of the true image, and with simple nearest-neighbour interpolation. While the more sophisticated method may be useful for more accurate color imaging, no difference

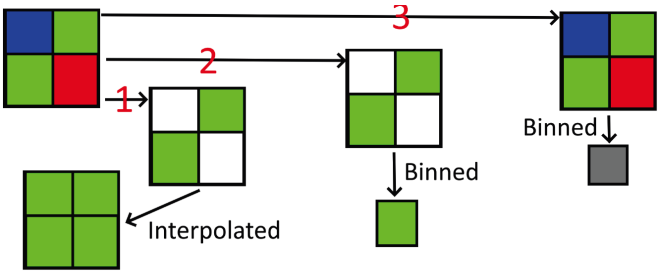

Figure 2. Visual representation of the three potential approaches to reducing the Bayer filter.

was perceptible between the two methods in terms of the quality of the photometry. The quality of the photometry was not great, unfortunately, as can be seen in Figure 3. In the well-exposed regime, there was clear variation between some stars where the interpolation worked relatively well—those with low variability—and those that did not, where the variety of scatter that is significantly above the common trend. The interpretation here is that those stars where the photometry worked well likely had most of their flux landing on "true" pixels whereas for those that did not work, much of the flux landed on interpolated pixels. The "hook" at the left hand of this graph and the following graphs is due to the saturation point of the 14-bit detector. The yellow dots represent the chosen comparison stars for the dataset. ASTROSOURCE (Fitzgerald 2018) chooses comparison stars using an algorithm that selects stars based on lowest variability within the dataset and a range of magnitudes. As the purpose of the study is the identification of variability, the comparison stars may be unique to each data set or even each dataset post processing. For example, the comparison stars identified by ASTROSOURCE in Figures 3, 4, and 5 are not the same stars. The comparison stars are stars chosen by ASTROSOURCE as having the lowest variability within the processed dataset. It is to be expected that different Bayer reduction methods will result in small differences in the experimentally measured variability of low variability stars leading to different comparison star selections.

It is worth noting that the horizontal axis is the difference of the mean magnitude of the given star to the ensemble magnitude of the selected comparison stars. As the primary interest is variability, the absolute values of the horizontal axis are not of particular significance to the study.

The second approach, collapsing the grid down into a lower resolution image for each color, fared better. In this approach, the variation for standard single stars dropped to about 0.049 typical variability per star with a minimum variability of 0.022 for stars between 2 and 3 mean differential magnitude, as can be seen in Figure 4.

The third approach, however, where the whole Bayer grid was collapsed—including all four real Bayer pixels—to a lower resolution image, provided the best quality photometry at about 0.043 median variability per star with a minimum variability of 0.024 for stars between 2 and 3 mean differential magnitude, as can be seen in Figure 5. While numerically the median and minimum variability do not vary so much between the second and third approaches, it is clear from visual inspection that the third approach is far superior.

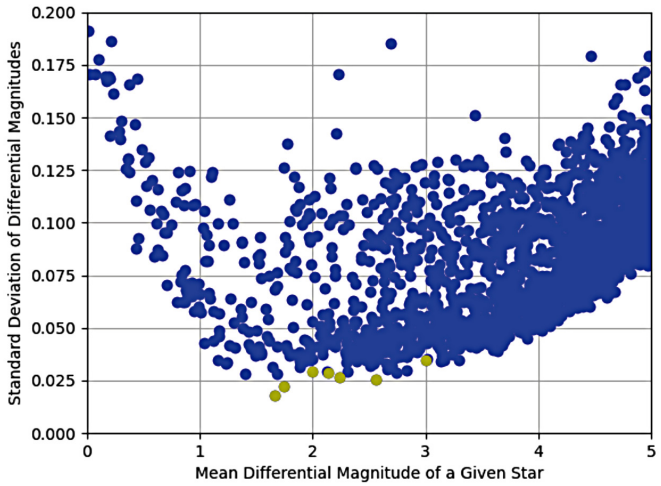

Figure 3. Internal differential photometry from interpolated color images. The yellow dots represent the chosen comparison stars for the dataset.

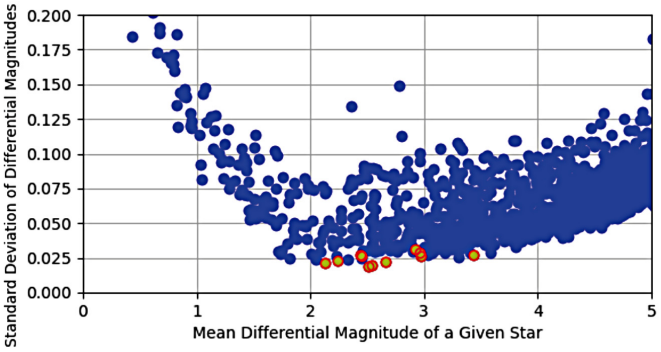

Figure 4. Internal differential photometry for collapsed color images only containing G pixels. The yellow dots represent the chosen comparison stars for the dataset.

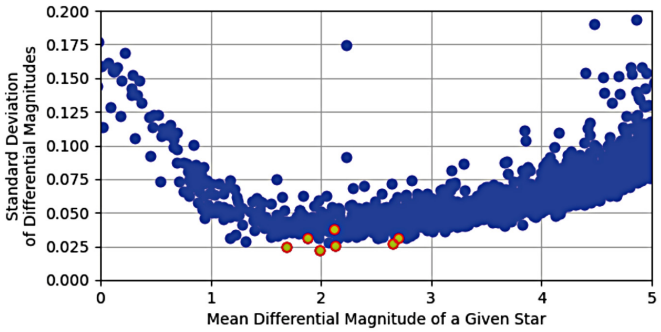

Figure 5. Internal differential photometry for the collapsed Bayer Grid containing all RGGB pixels. The yellow dots represent the chosen comparison stars for the dataset.

4.3. Calibrated photometry

The Bayer filters really are not a good match to any standard filter set and are primarily intended for color imaging rather than quality color photometry. Further complicating the issue here is that there was no UV/IR filter in front of the camera, meaning infrared light was also being captured unimpeded by the Bayer array—likely contributing to all pixels as OSCs can tend to have serious IR-leaks, as shown in the relative QE curve for this camera shown in Figure 6. As the goal of using the RASA was not to perform high quality calibrated color photometry but rather search for variables, it was decided that the collapsed Bayer grid, providing the best quality internal differential photometry as measured by standard deviation of variation, was the best option moving forward.

As there are two green pixels, one blue pixel, and one red pixel represented by each single "collapsed" pixel in these images, the images were interpreted as being a "CV" filter image. This is a clear filter reduced to V in AAVSO parlance. In a sense, given that there are two green contributing pixels and one blue and one red, it is likely somewhat closer to real V than a traditional clear filter but then perhaps less so due to the uncertain amount of infrared photons. The photometry of these images was calibrated to the APASS9 (Henden *et al.* 2016) catalogue using AstroSource. The color term was estimated to be –0.115 ± 0.021, which was the median color slope estimated from 475 frames which provided good color data. Using this as the standard value, the photometry was corrected to have a color term of 0.007 ± 0.031. Both of these color term distributions are shown in Figure 7. A sample of a single image's uncorrected and corrected color slope is shown in Figure 8.

The comparison between the calculated and catalogue magnitudes, shown in Figure 9, shows no systematic error, although a relatively wide scatter which is a combination of the RASA photometry errors as well as the APASS errors themselves. It can also be seen in the light curves presented in the results, that the agreement between the RASA calibrated photometry and ASAS-SN photometry (Shapee *et al.* 2014; Kochanek *et al.* 2017) is generally very good for the purposes of variable identification. If the pixel-scale was less blocky such that the internal differential photometry between the two methods was more comparable, it would be likely that we would have erred for just using the G pixels to increase the likelihood of matching to the standard system "V" filter, however for the purposes of this study, "CV" sufficed.

4.4. Finding variable stars

Once the data and CV calibration were adequately achieved, attention was drawn to finding the variables. The general principle of variable hunting was to analyze the full set of data over the whole observing season to identify stars in the images that were varying significantly above the general population of typical non-varying stars. AstroSource allows the identification of variation to be set at any level. AstroSource was set to identify stars that were varying more than two standard deviations above the mean variability of a 0.5 magnitude-wide bin. A 2-D histogram representing this data is shown in Figure 10; in this figure color is used to represent the number of stars observed within the colored block and blue dots are used to represent

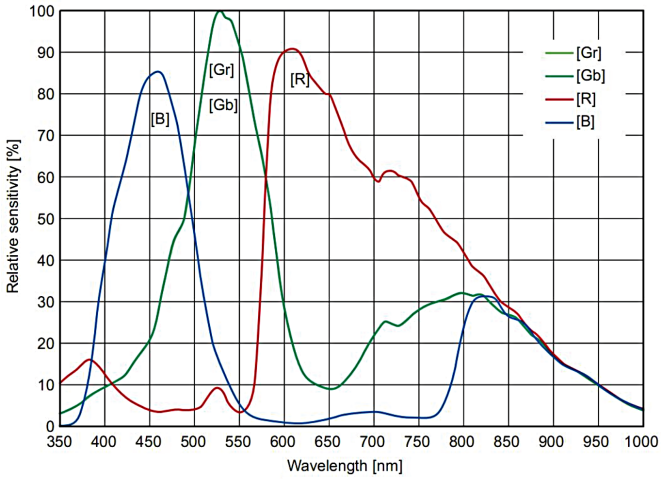

Figure 6. ZWO Relative QE curve for each of the Bayer pixels demonstrating the infrared light leak mentioned (Source: ZWO ASI071MC-Pro website: https://astronomy-imaging-camera.com/product/asi071mc-pro/).

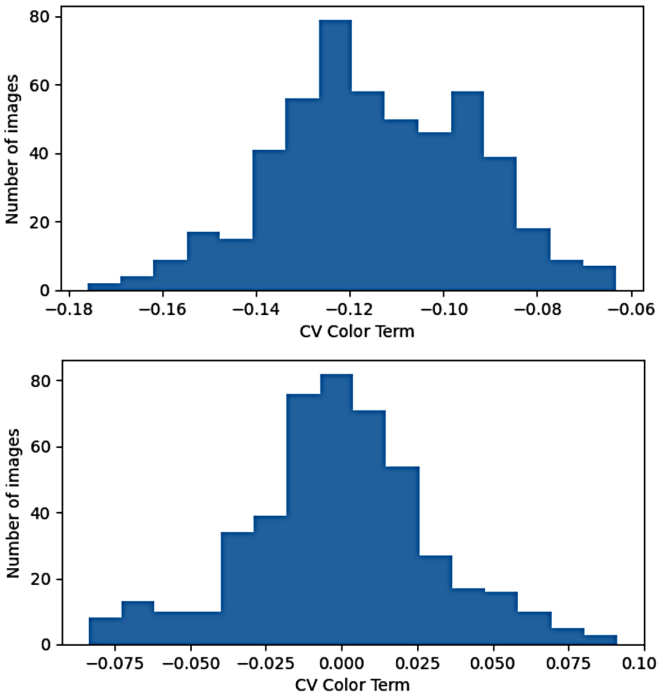

Figure 7. Before and after color term correction.

variable stars meeting the two-standard deviation criterion. Setting the variation limit a little low like this identified many more stars (approximately 100) than were truly variable. After these stars were identified, their light curves were folded on a best attempt at finding the period using multiple methods (PDM (Stellingwerf 1978), ANOVA (Schwarzenberg-Czerny 1989), Lomb-Scargle (Lomb 1976), and the string method (Dworestsky 1983), and were visually inspected by eye to identify those with a clear pattern to them. In future studies a 2.5-standard deviation criterion is suggested as a level that will reduce false positive identifications without reducing detection of true variables. It can be clearly seen in Figure 10 where there is a knee in the curve that the saturation level is at about 1 mean differential magnitude. This is roughly 10th mag, which means measurements nearing the level and above are not trustworthy.

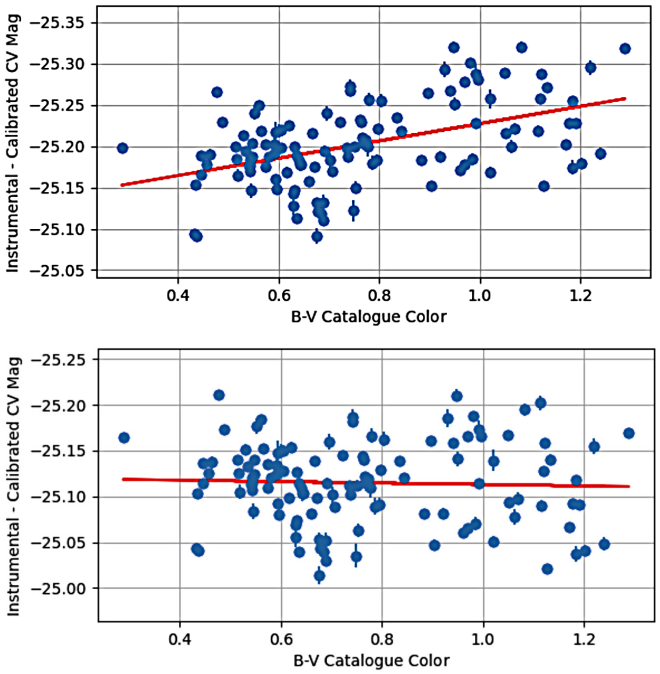

Figure 8. Difference in instrumental and calibrated magnitude before, and after, color correction for a single example image. Note, as a single value was used for all frames, representing the color term of the filter, the slope is not expected ever to be perfectly flat in the resultant corrected frame.

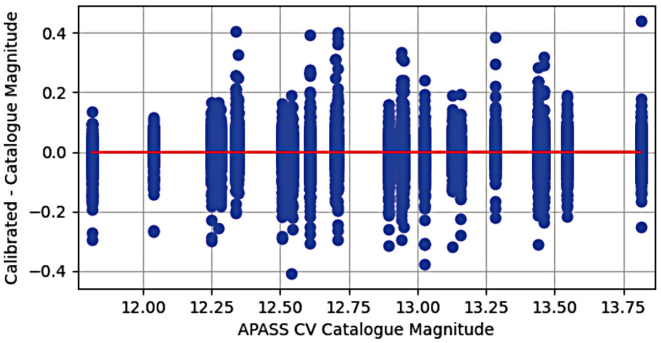

Figure 9. Comparison between calibrated magnitudes from the RASA and the catalogue magnitudes from APASS9.

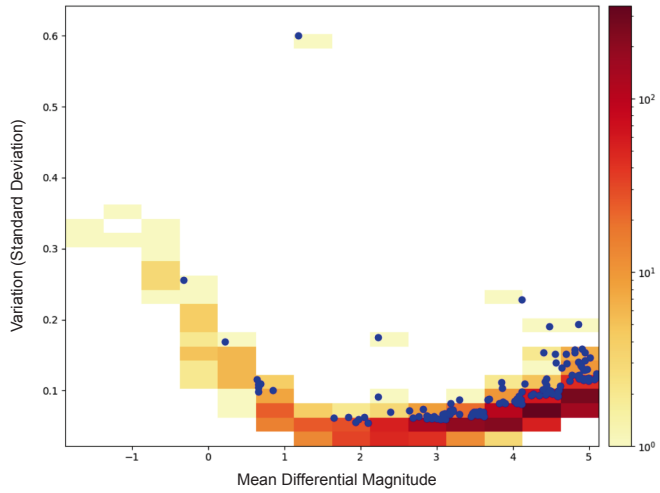

Figure 10. A two-dimension histogram of the variation across magnitudes in the dataset, where the blue dots indicate variation of two standard deviations above the mean—indicating potential variables.

5. Results

Three databases were used to obtain information on the identified variable stars: SIMBAD (Wenger *et al.* 2000), the AAVSO Variable Star Index (VSX; Watson *et al.* 2014), and the All-Sky Automated Survey for Supernovae (ASAS-SN, Shappee *et al.* 2014; Kochanek *et al.* 2017). SIMBAD is a dynamic database whose purpose is to "provide information on astronomical objects of interest which have been studied in scientific articles." SIMBAD provides all the basic information such as the coordinates, magnitudes, size, and identifiers. AAVSO VSX is a database whose purpose is to be a place where "all variable star data is made available to the general public, and through which the data is maintained, revised, and commented upon." ASAS-SN is an all-sky survey looking for supernovae which contains similar blocky pixel-scale clear V APASS calibrated photometry that we used as a comparison for the RASA photometry.

There is a significant difference between the collection methodology for this study's RASA data and the ASAS-SN data. The ASAS-SN data are single points taken over a decade. The RASA data are all within a few weeks of each other, with imaging sessions typically 20 to 60 minutes per night. Period calculations using the ASAS-SN data for short period variables may be less reliable than the RASA data. Additionally, consideration should be given to small changes in period that may be occurring over years or decades that will affect ASAS-SN data.

Over the observing period 12 variable stars were identified using the statistical analysis software. As has been discussed, our method of finding these stars relied on an independent method which was then compared to the results from AAVSO VSX, ASAS-SN, and SIMBAD. The main period-finding technique we used was the ANOVA technique (Schwarzenberg-Czerny 1989), which seemed to find periods in this dataset more clearly than other techniques. The 12 variable stars identified are listed in Table 2. We discuss each of the 12 variables in more detail below; distances provided are all from GAIA DR3 (Bailer-Jones *et al.* 2021).

The following light curves (from the RASA) are split through blue and red for ease of viewing and interpretation, with the blue showing the first period and red the second period.

5.1. EC-01

Located at R.A. 154.5431°, Dec. –34.6327° (J2000), EC-01 is an already confirmed eclipsing binary variable star with a period of 0.288 day listed in the AAVSO VSX as SSS_J101810.3-343758 and is found 542 parsecs away. EC-01 has a dimmest magnitude of 15 V and a brightest magnitude of 14 V. Figure 11 presents the RASA and ASAS-SN light curves for comparison. This variable was first identified in the Catalina Surveys Southern (CSS) periodic variable star catalogue (Drake *et al.* 2017), followed closely by the first catalogue of variable stars measured by the Asteroid Terrestrial-impact Last Alert System (ATLAS, Heinze *et al.* 2018). The general fluctuation of the ASAS-SN light curve is similar to the one that we had received from the RASA. Alongside this, the magnitude range for both EC-01 and the light curve from ASAS-SN match up to be around the same, with the inclusion of the few outliers.

Table 2: Identified variable stars in this study.

Internal Name (External Name)	*R.A. (°) (J2000)*	*Dec. (°) (J2000)*	*Magnitude Range*	*Estimated Period*	*Prior Reported Period*	*Type*
EC-01 (SSS_J101810.3-343758)	154.5431	–34.6327	14–15 V	0.288d	0.288d	Eclipsing BSinary
EC-02 (SSS_J101835.0-345553)	154.6461	–34.9312	14.4–15.2 V	0.3348d	0.334894d	Eclipsing Binary
EC-03 (ASAS J101909-3423.0)	154.7857	–34.3841	10.6–11.0 V	0.35d or 9.67d	9.668d (MNRAS 2009)	Rotational Variable
EC-04 (CD-34 6620)	154.8340	–35.0109	10.6–10.9 V	Uncertain	Not reported as variable	Potential Rotational Variable
EC-05 (TYC 7191-2279-1)	155.1041	–34.4157	10.7–11 V	Uncertain	Not reported as variable	Unknown
EC-06 (AP42560121 no entry in SIMBAD)	155.1971997	–34.294665	13.5–14.0 V	Uncertain, possibly 0.167d	Not reported as variable	Unknown
EC-07 (AC Ant)	155.386	–34.659	10.25–12 V (our data), 10.9–15.2 V	Not determinable	212.86	Mira
EC-08 (SSS_J102337.5-344807)	155.9057	–34.8018	14.7–15.4 V (ASAS-SN)	0.2668d	0.26888d	Eclipsing Binary
EC-09 (AP42549399 no entry in SIMBAD)	156.0172	–34.5487	15.5–16.0 V	Approximately 0.35d	Not reported as variable	Potential RRc RR-Lyrae
EC-10 (ASAS J102405.1-344145)	156.0211	–34.6955	12.8–12.3 V	Unclear! Either 0.4153d (RASA) or 0.368d (ASAS-SN)	0.368265d	Eclipsing Binary
EC-11 (SSS_J102414.5-345424)	156.0604191	–34.9069155	16.0–15.3 V	0.43486d	0.430632d	Eclipsing Binary
EC-12 (Gaia DR3 5445972871533753088 no entry in SIMBAD)	156.1388205	–34.3688099	15.7–16.2 V	0.0834d	Not reported as variable	Potential δ Scuti / SX Phe

5.2. EC-02

EC-02 is found at R.A. 154.6461°, Dec. –34.9312° (J2000), and is identified in AAVSO VSX as SSS_J101835.0-345553, an eclipsing binary star system located 819 parsecs away. EC-02 has a period of 0.3348 day, a brightest magnitude of 14.2 V, and a dimmest magnitude of 15.1 V. The RASA and ASAS-SN light curves are shown in Figure 12. SSS_J101835.0-345553 was also identified in the CSS and ATLAS surveys as similar to EC-01. As can be easily seen, the light curves are similar despite the RASA light curve being more patchy and is more clumped with more outliers.

5.3. EC-03

Located at R.A. 154.7857°, Dec. –34.3841° (J2000), EC-03 was detected with an initial period of 0.35 day, a dimmest magnitude of 11.1 V, and a brightest magnitude of 10.5 V, and is located 635 parsecs away. EC-03 is referred to as ASAS J101909-3423.0 in VSX as an eclipsing binary star with a 9.67-day period and further analysis was conducted with this period. The star is potentially bright enough to be affected by sensor saturation leading to the unusually large noise measured in the light curves shown below in Figure 13. EC-03 (ASAS J101909-3423.0) was identified by the All Sky Automated Survey (ASAS; Pojmański 2002) and was later followed-up in the Spectroscopic Survey of ASAS eclipsing variables (Parihar *et al.* 2009). ASAS-SN identifies it as a Rotational variable, ASASSN-V J101908.59-342302.4. The RASA data folded on the period identified provide a believable curve for this period, as does a reprocessing of the ASAS-SN data—both shown in Figure 14. However, the length of the period would not have been independently discoverable in this dataset due to the period length compared to the time base of the data.

5.4. EC-04

EC-04 is located at R.A. 154.834°, Dec. –35.0109° (J2000), and is known as CD-34 6620 in SIMBAD, is not listed as a variable star there or in VSX, and is not identified as a variable star in ASAS-SN. EC-04 is located around 133 parsecs away. EC-04 was detected with a possible period of 0.355 day with significant doubt, upon further inspection, it looked like strips of multiple periods were layered on top of each other. A further search for a longer period identified two possible spikes in the periodogram, however it is inconclusive due to the significant patchiness of the data for longer periods. While viewing the data we had for this star, we saw that it seemed similar to EC-03, where it is potentially a rotational variable. However, the time base—again—of the RASA data does not allow us to confirm this. The minimum magnitude of this variable approaches but does not exceed the saturation magnitude of this method. Exploring the ASAS-SN data, there is some clear variation over a similar magnitude range on the longer term that we see in the RASA.

There is a nearby star roughly 20 arcseconds away that is 2.5 magnitudes dimmer than this star. While it is possible that the nearby star is affecting the measurements, it is roughly 10–20% the brightness of this target star. As the pixel scale is somewhat blocky—although the apertures are much smaller than this (roughly 2–3 arcseconds)—this is a possible contributor to measured variation. However, the ASAS-SN data also show a distinct systemic change at the 0.1-mag level. Hence, the variability is uncertain. The star also has a brightest magnitude of 10.6 V and a dimmest magnitude of 11.0 V. The light curves are shown in Figure 15.

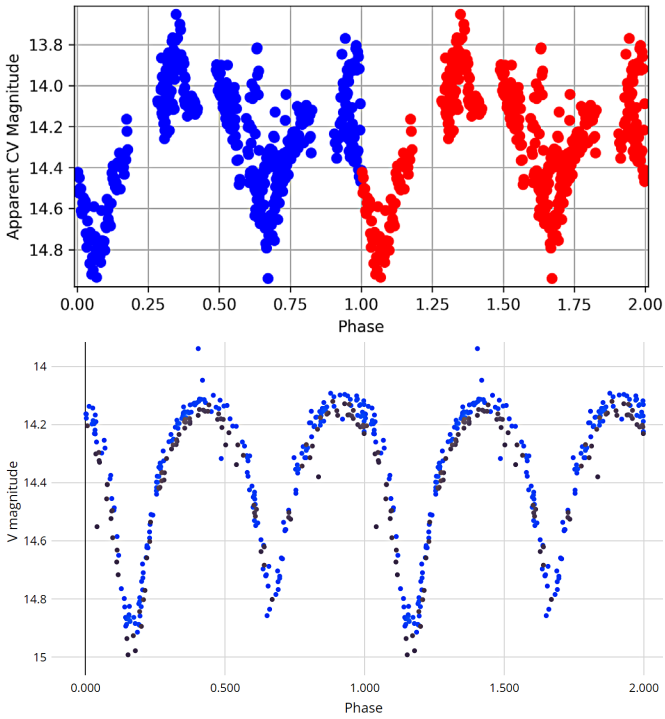

Figure 11. RASA (top) and ASAS-SN (bottom) light curves of EC-01.

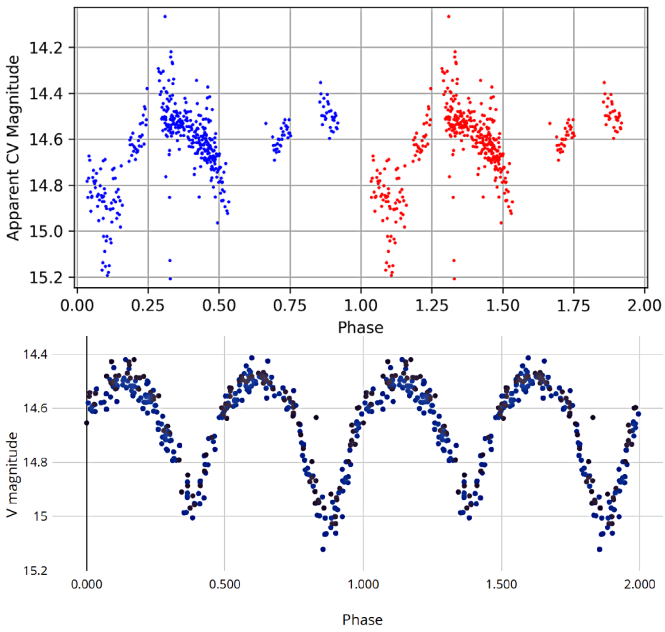

Figure 12. RASA (top) and ASAS-SN (bottom) light curves for EC-02.

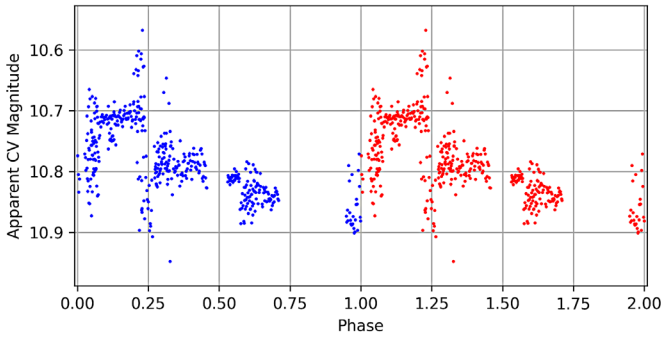

Figure 13. Initial RASA light curve for EC-03.

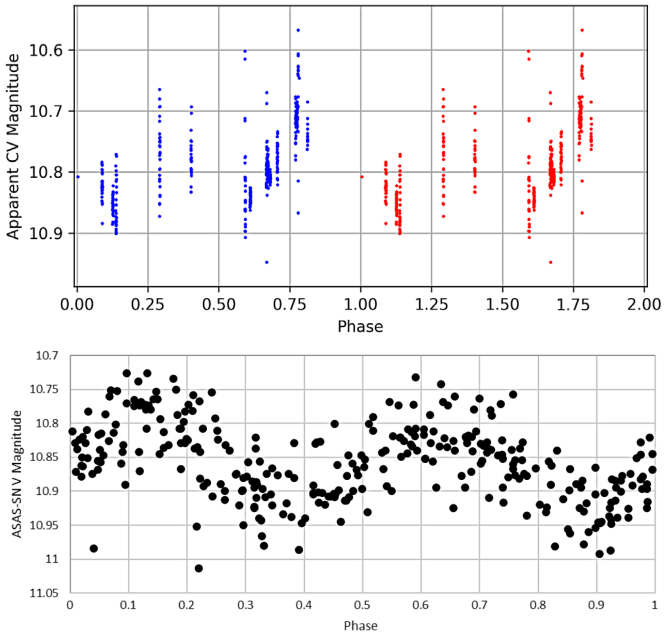

Figure 14. RASA (top) and ASAS-SN (bottom) EC-03 photometry both folded on a 9.67-day period.

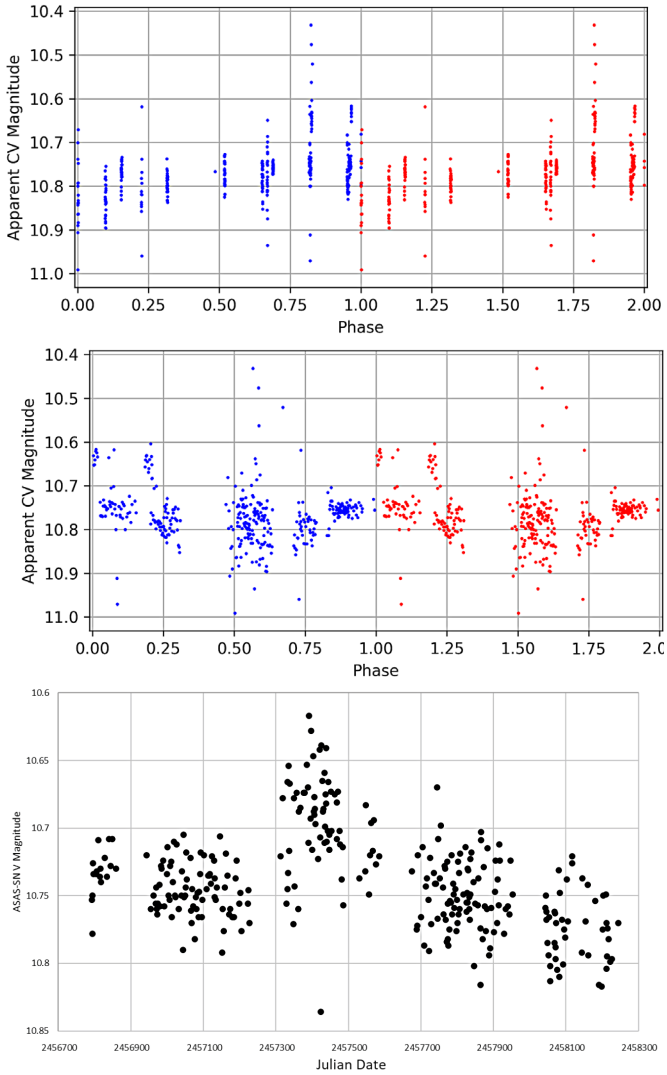

Figure 15. Potential variation periods for EC-04 for two periods from the RASA (top and middle) and the non-folded raw data straight from ASAS-SN.

5.5. EC-05

Located at R.A. 155.10415°, Dec. –34.4157° (J2000), EC-05 is referred to in SIMBAD as TYC 7191-2279-1. EC-05 is located around 2371 parsecs away. There are no mentions of variability for this star in SIMBAD or VSX. The star has a brightest magnitude of 10.7 V and a dimmest magnitude of 11.0 V. The periodicity of the star was inconclusive, but there is clear variability. The RASA light curve, folded on an arbitrary period to display multiple nights' data, is shown in Figure 16. This star is found in ASAS-SN but has a slightly different magnitude than what we have recorded, where the dimmest magnitude was about 10.95. In ASAS-SN, the light curve looks quite different, being quite flat while also being about 0.3 magnitude dimmer.

5.6. EC-06

Located at R.A. 155.197199°, Dec. –34.294665° (J2000), EC-06 has a brightest magnitude of 13.5 V and a dimmest magnitude of 14.0 V and is at a distance of 689 parsecs. We found EC-06 had a potential period of 0.164 or 0.167 day, using the RASA and LCO data, respectively (Figure 17a). There are no current variables in AAVSO VSX near this star. This period is visible in both the RASA data and follow-up LCO data, as can be seen in the light curve in Figure 17a. However, it cannot be seen in the ASAS-SN data. The variation itself is likely, as the variation is seen with two quite distinctly separate telescope systems, however the nature of the object is uncertain.We also explored a wider range of potential periods and found a potential likely period of roughly 3.85 days (Figure 17b), however, the nature of the time base of the RASA data means this is only indicative at best.

5.7. EC-07

EC-07, or V* AC Ant, as referred to in SIMBAD (the V* means variable star), is a Mira variable star which coordinates are R.A. 155.3864°, Dec. –34.659° (J2000). AC Ant is located around 5430 parsecs away. The period of this Mira is 212.89 days (Vogt *et al.* 2016). As the period is longer than our observing period we could not independently measure the period of this star and make no claims in this respect. It looks like we captured the star at its brightest and it decreased in brightness over our observing period, as shown in Figure 18. Our estimation of its peak brightness is significantly brighter than the ASAS-SN magnitude, but without a full light curve we cannot say much more. However, Mira variables are extremely red, which could interact poorly with our "clear V" filter measurements particularly if the OSC was sensitive to IR-leaks. It is also the case that the Mira was by far the brightest variable we identified and may suffer from non-linearity effects from the more limited 14-bit dynamic range. On ASAS-SN's side, 11th magnitude is the saturation limit, so the ASAS-SN light curve itself may be curtailed. It is likely that the star's very red color, when observed with the RASA camera (which has a known sensitivity to red and near IR light), could have affected the measurements of magnitude. To be short, these magnitudes are not to be trusted! Given the primary purpose of the study—to identify variable stars—it is a confirmation of the method that even a comparatively long period variable has been detected.

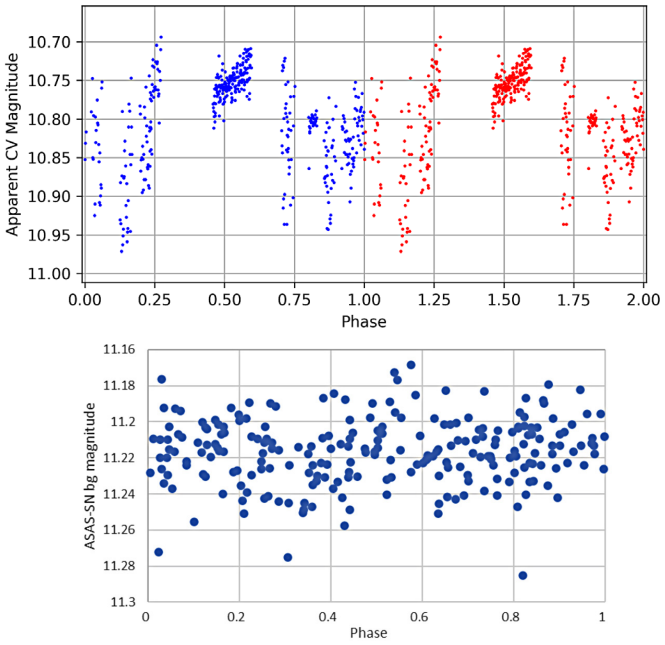

Figure 16. Variation detected in the RASA photometry (top) and ASAS-SN photometry (bottom), folded on an arbitrary period for EC-05.

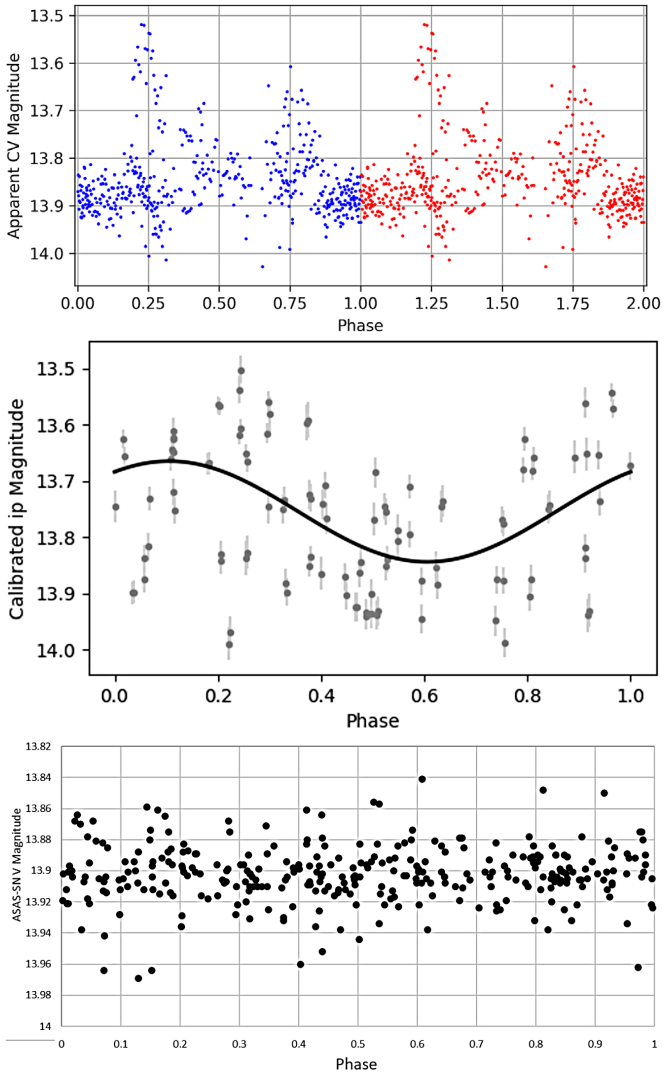

Figure 17a. RASA folded photometry (top), LCO folded photometry (middle), and ASAS-SN folded photometry (bottom) light curves of EC-06 on a 0.167-d period.

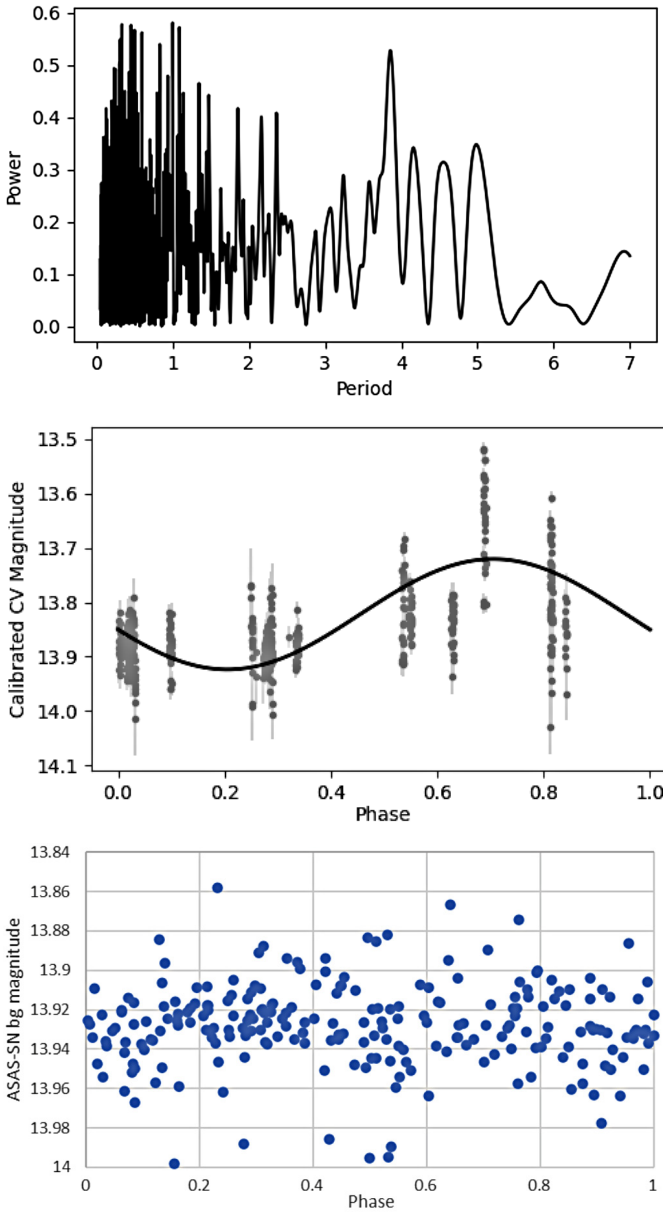

Figure 17b. Results from a wider search for variability showing a potential 3.85-d period in EC-06. This is not clear in the ASAS-SN data.

5.8. EC-08

EC-08, or CRTS J102337.5-344807, as referred to in SIMBAD, is located at R.A. 155.9057°, Dec. –34.8018° (J2000), and is located approximately 428 parsecs away. As shown in Figure 19, the dimmest magnitude is 15.4 V, and the brightest magnitude is 14.7 V. VSX shows this star to be an EW Eclipsing Binary. The RASA and ASAS-SN light curves for this star are shown in Figure 19. The comparison of the two immediately highlights how the light curve for EC-08 is incomplete, with sections that are shown in the ASAS-SN light curve missing from the EC-08. Apart from those major sections that are missing, what we have from the EC-08 light curve can easily fit into the one from ASAS-SN.

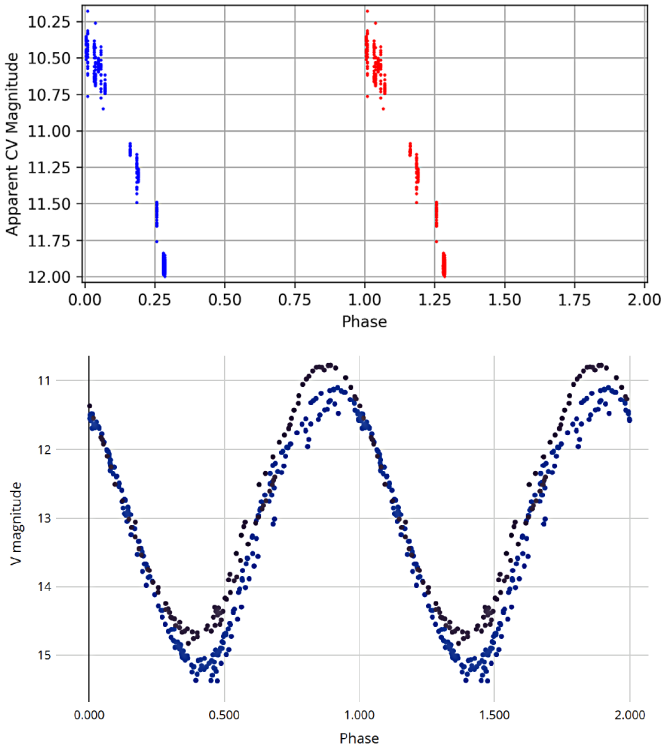

Figure 18. RASA (top) and ASAS-SN (bottom) data folded on known period for AC Ant. The ASAS-SN data include measurements from two separate instruments superimposed (blue and grey points).

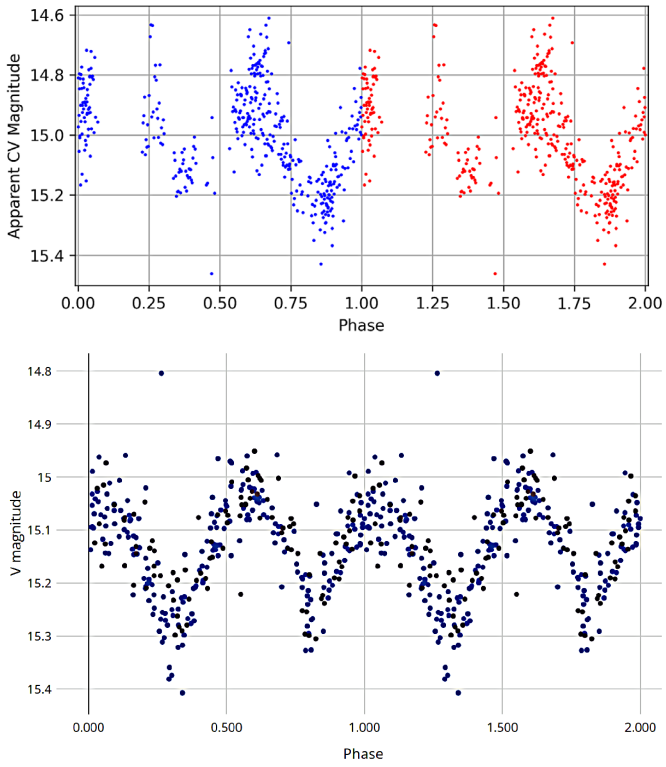

Figure 19. RASA (top) and ASAS-SN (bottom) phased light curves for EC-08.

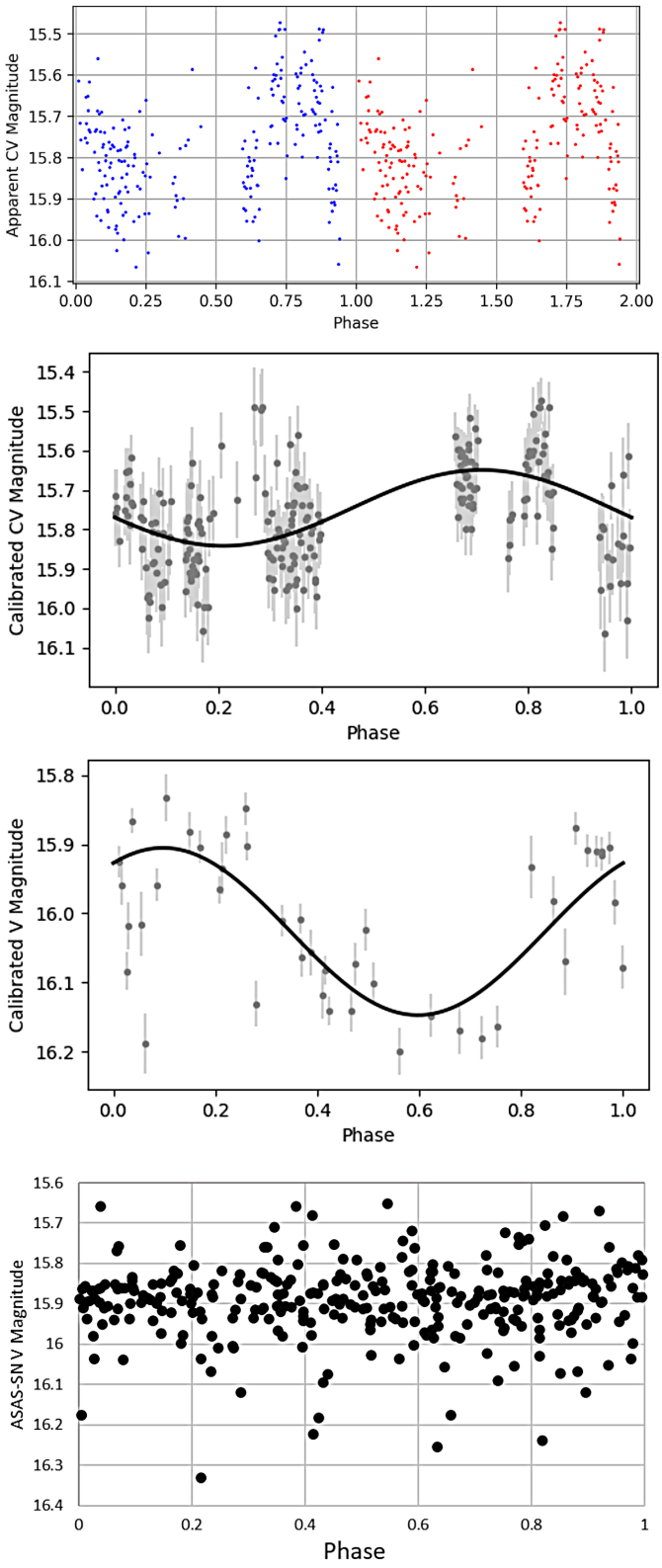

Figure 20. RASA photometry of EC-09 folded on ANOVA detected period (top), RASA photometry folded on Lomb-Scargle period (second), LCO photometry folded on ANOVA detected period (third), ASAS-SN photometry folded on 0.35 days (bottom).

5.9. EC-09

EC-09 is a variable star located at R.A. 156.0172°, Dec. –34.5487°, at a distance of 1174 parsecs. According to the light curve below (Figure 20), it has a dimmest magnitude of 16.1 V, and a brightest magnitude of 15.5 V. Follow-up observations from LCO showed a similar pattern with a similar period and similar magnitudes, as did multiple period techniques, including a Lomb-Scargle technique which identified a similar period. The nature of this star is not conclusive due to the patchiness of data. However, it is likely an RRc-type RR-Lyrae because of its relatively low (0.3 mag) amplitude and seemingly smooth sinusoidal pattern over a potential period from of between 0.33 and 0.37 day, but we are unable to confirm anything as of yet. The star is clearly variable but a complete and plausible period could not be found. Neither VSX nor SIMBAD includes this star within their databases. The light curve, as generated by our data, is shown in Figure 20, as are light curves from LCO and ASAS-SN data. ASAS-SN data folded on the general range of periods 0.33 to 0.37 d show no periodicity, but the scatter in the ASAS-SN data at this dim magnitude is quite high.

5.10. EC-10

EC-10, located at R.A. 156.0211°, Dec. –34.6955°, is a previously identified eclipsing binary (Pojmański 2002) and is 476 parsecs away. It is referred to in SIMBAD as ASAS J102405-3441.7. It has a dimmest magnitude of 12.8 V and a brightest magnitude of 12.3 V. VSX provides a period of 0.368273 d, however, this does not create a believable light curve with the RASA data. The period found by our analysis (0.2256 d) displays a tight, reasonable light curve—presumably half the period of a fairly symmetrical eclipsing binary. Twice the period (0.4513 d) also provides a believable, if patchy, double eclipse light curve.

The magnitude ranges from this study, from ASAS-SN and from the earlier ASAS-3 survey (Pojmański and Maciejewski 2004) are in broad agreement. However we did not find agreement with the reported VSX (V band) magnitude range which we were unable to rationalise.

ASAS-SN and VSX both provide a full period of 0.368 d. Folding the RASA data on half the VSX period (0.184 d) or the full VSX period (0.368 d) does not create a believable light curve, yet folding the ASAS-SN data on the RASA period only provides what seems to be random scatter. The light curves are shown in Figure 21.

These results appear irreconcilable. The researchers have re-confirmed the coordinates of the subject star and conclude that either there is an identification error that the researchers have not detected, or ASAS-SN has incorrectly identified the star (or there is a data mix-up), or the period of this eclipsing binary has changed substantially since the ASAS-SN data were collected. This star requires follow-up.

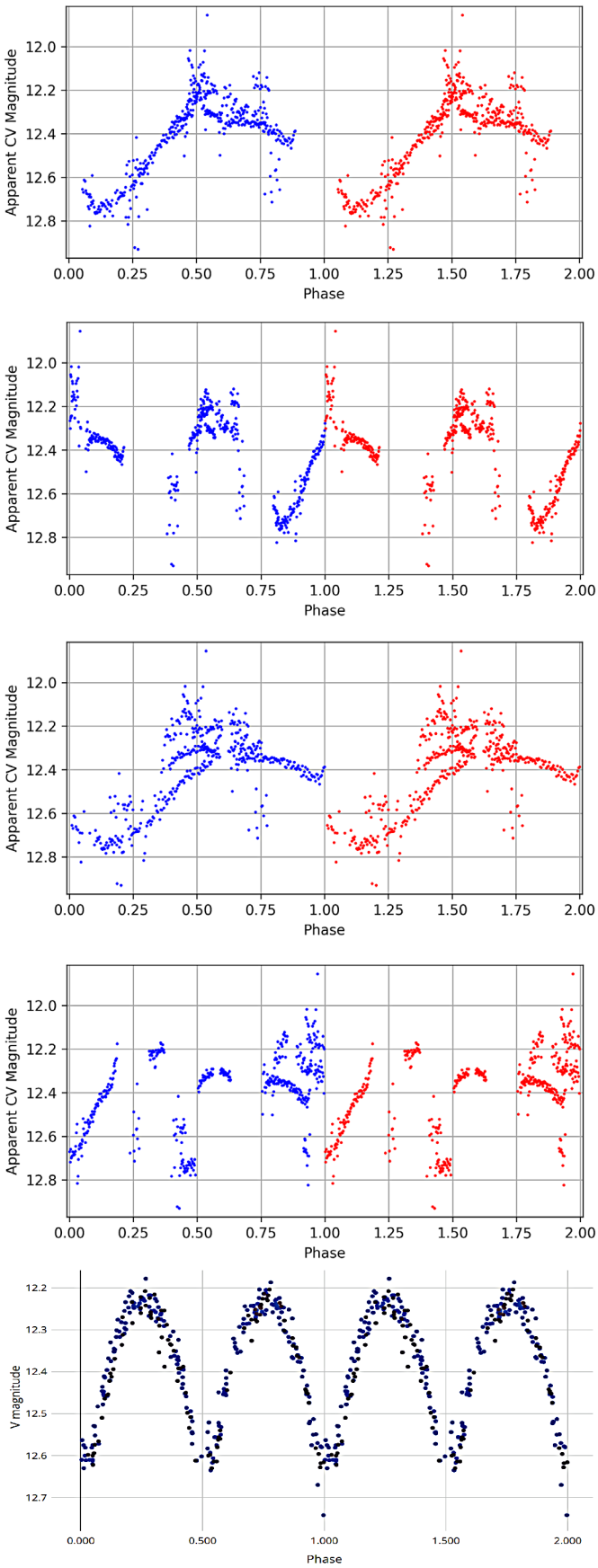

Figure 21. RASA photometry phased on trial periods of 0.2256 d, 0.4513 d, 0.184137 d, and 0.368273 d, respectively (top four), compared to ASAS-SN data on trial period of 0.368 d (bottom).

5.11. EC-11

EC-11, referred to in SIMBAD as SSS_J102414.5-345424, is a previously identified eclipsing binary whose coordinates are R.A. 156.060419°, Dec. –34.906915°, and is located around 2500 parsecs away. The star has a faintest magnitude of 16.2 Vand a brightest magnitude of 15.2 V, according to our light curve shown in Figure 22.

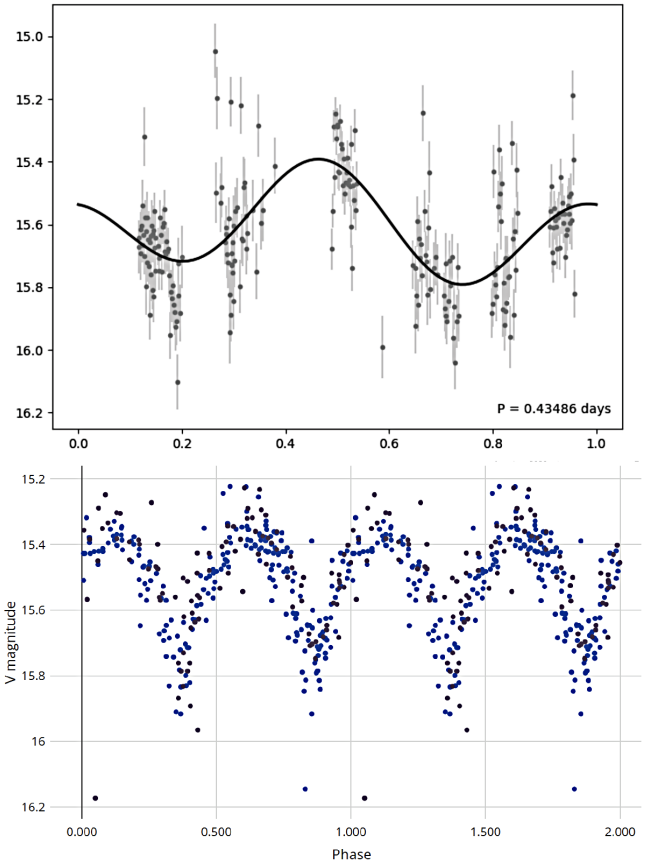

Figure 22. EC-11 RASA folded photometry based on Lomb-Scargle method (top), ASAS-SN folded photometry (bottom) on known period 0.43486 d.

5.12. EC-12

EC-12 is located at R.A. 156.138821°, Dec. –34.368810° at a distance of 823 parsecs. When looking at the light curves in Figure 23, it is easy to see that there is a clear repeating pattern taking place in both the RASA and some follow-up LCO data roughly over a 0.082-day period. Examining the ASAS-SN data folded on 0.082 d shows no trend, although visually it appears that at this dimness (15.8 V to 16.5 V magnitude), the scatter in the ASAS-SN data is larger than the variation we see. The shape of the light curve and the very short period indicates it is likely a δ Scuti or SX Phe type variable.

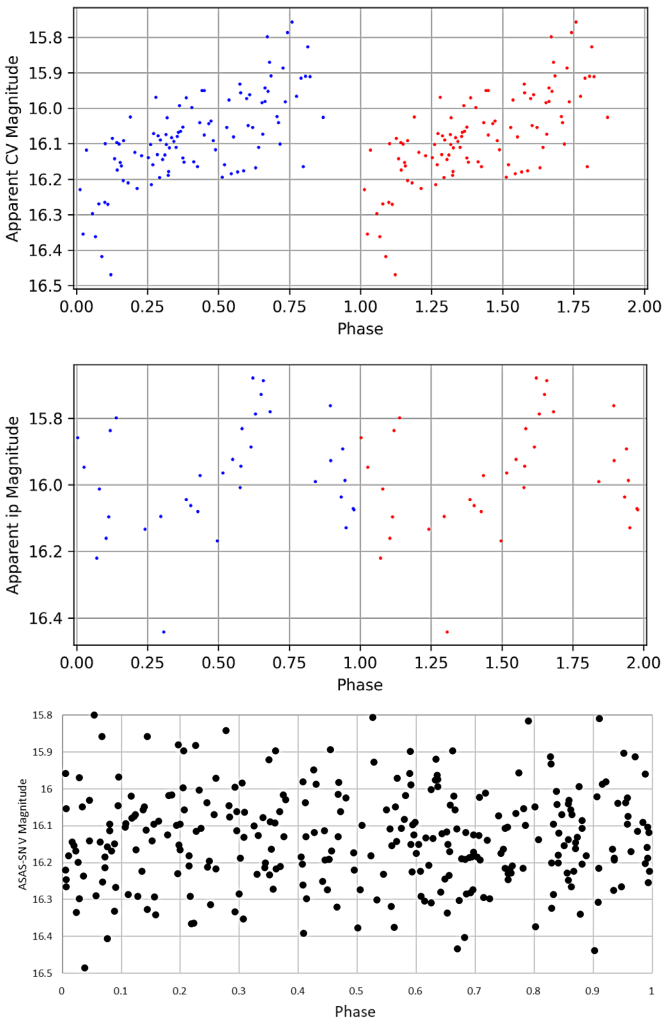

Figure 23. RASA(top), LCO (middle), and ASAS-SN (bottom) phased photometry light curves of EC-12 based around detected period of approximately 0.082 day.

6. Discussion

It can be seen from the findings above that the combination of a wide-field RASA 11-inch telescope with a mid-level OSC camera can lead to substantial discoveries when used as a variable-hunting telescope. Aside from selecting an area of the sky seemingly low in variable stars from the AAVSO, no reference to known variables was used in the identified variables in this paper. The team identified the variables within the dataset and then went to the online databases, primarily AAVSO VSX, ASAS-SN, and SIMBAD to identify whether or not these were previously known variables.

The resolution of the telescope was relatively low (1.6 arcseconds/bayer pixel, 3.2 arcseconds/binned pixel). The match between a standard V filter and the "clear V" binned Bayer filter array is not great (–0.101 color term) and not to be trusted as a measurement of a true "V" measurement as, realistically, it is an "air" filter that includes uncontrolled amounts of blue, red, and infrared light as well. Despite this, a serviceable approximation of the V magnitude was achieved and was certainly good enough for identification purposes. Internally, the photometry system provided good results internally with a range of 0.02–0.05 mag error at the brightest end of the usable range down to about 0.07–0.1 at the dimmest range considered. As can be seen in EC-12 and EC-09, good results were achieved down to 16.5th mag and 16th mag, respectively. The other brighter magnitude identifications all showed clear signal. This was all with a relatively short 60s exposure time with a somewhat limited 14-bit dynamic range with essentially an "air" filter. To really pin down the actual periods of the discoveries, many more nights—perhaps double (28)—were required to achieve good randomized coverage for a range of potential trial periods. Many of the identified variables show blank patches in their light curves.

The observatory has recently been loaned a QHY600C Pro camera by the Photon Ranch project through Las Cumbres Observatory, improving the pixel scale from 1.6 asec/pix to 1.25 asec/pix, boosting the dynamic range to 16-bit and roughly—but not quite—doubling the field of view to about 4 × 3 degrees. Also, a UV/IR cut filter is being used to prevent IR leakage into the Bayer array, which may prevent wildly divergent magnitude measurements for very blue and very red stars—such as the identified Mira—at the cost of some throughput. With the new camera and the learnings made in this project, another test search will be undertaken this year to further trial this variable search methodology. This time, it will approach the problem from a different direction: In a field rich with variables, how deep can the equipment search in magnitude, what percentage of known variables will it recover, and how many new variables will be discovered? It is likely to reach beyond the dim end of ASAS-SN (roughly 17th magnitude) with a superior pixel-scale (1.25 arcsec per bayer pixel or 2.5 arcsec per binned pixel compared to 8 arcsec/pixel for ASAS-SN). We also will be following-up our discoveries in this paper with a co-located CDK17 with SBIG16803 camera this year. It is clear that there are discoveries to be made beyond 15th magnitude with such wide-field equipment.

7. Conclusion

This process took place over the course of about a year and through this time we have been able to confirm the variability of 12 stars in a field of view in the constellation of Antlia. Five of these (EC-04, EC-05, EC-06, EC-09, EC-12) did not have any previous records for being variable. Using SIMBAD, VSX, and ASAS-SN we were able to confirm these stars as previously identified or as new potential discoveries. The new potential discoveries were a likely rotational variable, likely RRc RR-Lyrae variable, likely δ Scuti/SX Phe-type variable, and two stars of unknown type. These potential discoveries will be followed-up with further research.

8. Acknowledgements

This research has made use of the SIMBAD database, operated at CDS, Strasbourg, France. This work makes use of observations from the Las Cumbres Observatory global telescope network and the ASAS-SN network. This paper makes use of data from the AAVSO Photometric All Sky Survey (APASS), whose funding has been provided by the Robert Martin Ayers Sciences Fund and from the NSF (AST-1412587). This research made use of the AAVSO Variable Star Index (VSX).

References

Bailer-Jones, C. A. L., Rybizki, J., Fouesneau, M., Demleitner, M., and Andrae, R. 2021, *Astron. J.*, **161**, 147.

Bertin, E., and Arnouts, S. 1996, *Astron. Astrophys., Suppl. Ser.*, **117**, 393.

Bortle, J. E. 2001, "Introducing the Bortle Dark-Sky Scale," *Sky and Telescope*, **101**, 126.

Breus, V. V. 2017, *Adv. Astron. Space Phys.*, **7**, 3.

Brown, T. M., *et al.* 2013, *Publ. Astron. Soc. Pacific*, **125**, 1031.

Drake, A. J., *et al.* 2017, *Mon. Not. Roy. Astron. Soc.*, **469**, 3688.

Dworetsky, M. M. 1983, *Mon. Not. Roy. Astron. Soc.*, **203**, 917.

Fitzgerald, M. T. 2018, *Robotic Telesc. Student Res. Education Proc.*, **1**, 347.

Fitzgerald, M. T., Gomez, E., Salimpour, S., Singleton, J., and Wibowo, R. W. 2021, *J. Open Source Software*, **6**, 2641.

Heinze, A. N., *et al.* 2018, *Astron. J.*, **156**, 241.

Henden, A. A., Templeton, M., Terrell, D., Smith, T. C., Levine, S., and Welch, D. 2016, VizieR Online Data Catalog: AAVSO Photometric All Sky Survey (APASS) DR9, II/336.

Kochanek, C. S., *et al.* 2017, *Publ. Astron. Soc. Pacific*, **129**, 104502.

Lomb, N. R. 1976, *Astrophys. Space Sci.*, **39**, 447.

Menon, D., Andriani, S., and Calvagno, G. 2007, *IEEE Trans. Image Processing*, **16**, 132.

Motl, D., 2021, C-Munipack software utilities (http://c-munipack.sourceforge.net).

Parihar, P., Messina, S., Bama, P., Medhi, B. J., Muneer, S., Velu, C., and Ahmad, A. 2009, *Mon. Not. Roy. Astron. Soc.*, **395**, 593.

Pojmański, G. 2002, *Acta Astron.*, **52**, 397.

Pojmański, G., and Maciejewski, G. 2004, *Acta Astron.*, **54**, 153.

Schwarzenberg-Czerny, A. 1989, *Mon. Not. Roy. Astron. Soc.*, **241**, 153.

Shappee, B., *et al.* 2014, *Amer. Astron. Soc. Meeting Abstracts*, **223**, 236.

Stamp, W. 2016, "Searching for a Variable Star" (poster presentation, Astronomical Society of Victoria, Junior Section), Melbourne, Australia.

Stellingwerf, R. F. 1978, *Astrophys. J.*, **224**, 953.

Vogt, N., *et al.* 2016, *Astrophys. J., Suppl. Ser.*, **227**, 6.

Waagen, E. O. 2022, "Variables: What Are They and Why Observe Them?"[1]

Watson, C., Henden, A. A., and Price, C. A. 2014, AAVSO International Variable Star Index VSX (Watson+, 2006–2014; https://www.aavso.org/vsx).

Wenger, M., *et al.* 2000, *Astron. Astophys., Suppl. Ser.*, **143**, 9.

[1] Waagen (2022), (https://www.aavso.org/variables-what-are-they-why-observe-them)